

Spontaneous Formation of Hierarchical Macro–Mesoporous Ethane–Silica Monolith

Kazuki Nakanishi,^{*,†,§} Yuki Kobayashi,[†] Tomohiko Amatani,[†]
Kazuyuki Hirao,[†] and Tetsuya Kodaira^{‡,§}

Department of Material Chemistry, Graduate School of Engineering, Kyoto University,
Nishikyo-ku, Kyoto 615-8510, Japan, and Nanoarchitectonics Research Center, National
Institute of Science and Technology, 1-1-1, Higashi, Tsukuba-shi, Ibaraki 305-8565, Japan

Received April 28, 2004. Revised Manuscript Received June 11, 2004

Monolithic ethane–silica gels with well-defined co-continuous macropores and highly ordered mesopores have been synthesized via a spontaneous route from silicon alkoxide with the aid of a structure-directing agent. While the macropores are formed by the concurrent phase separation and sol–gel transition induced by the polymerization reaction, the mesopores are templated by the self-organization of the structure-directing agent. Starting from a homogeneous mixture of the starting components, all the structure formation processes take place spontaneously in closed conditions at a constant temperature. Subsequent evaporation drying and heat treatment result in gels with hierarchical and fully accessible pores in discrete size ranges of micrometer and nanometer. While the local alignment of the mesopores is confirmed by FE-SEM observation, the long-range mesoscale order over the whole sample is evidenced by X-ray diffraction measurements. With the addition of a micelle-swelling agent, the mesostructural transition from 2D-hexagonal order to mesostructured cellular foam, MCF, has been observed without disturbing the macroporous framework structure.

Introduction

After the first synthesis of oxides with highly ordered mesopores templated by structure-directing agents,^{1,2} it has long been a tough challenge in sol–gel materials to combine the highly ordered mesostructures with well-defined co-continuous macropores based on phase separation.³ Mesoporous materials with a wide variation in chemical composition are now available in the forms of fine powder, thin film, and particles with controlled size and shape, and even in monoliths. For the purpose of fully utilizing the mesopore surfaces, however, their integration into a well-defined supporting structure is crucial. Especially in the case of liquid-phase reactions, the material transport path has to be designed so as to enhance the diffusional access of guest molecules to the reactive sites. It has been well-accepted that silica gels with continuous macropores synthesized via the phase-separation route perform much better than conventional particle-packed structure in HPLC separations.⁴ It is, therefore, expected that by embedding highly ordered

mesopores in the gel skeletons constituting the well-defined macroporous framework, a highly efficient liquid-phase contact device suitable for separation, reaction, and sensing purposes, can be prepared.

In most practices, highly ordered mesoporous materials are synthesized in dilute conditions with water-rich solvents. Started from metal alkoxides, the solvent mixture inevitably contains short-chain alcohols generated by the hydrolysis reaction. Unless selectively removed, short-chain alcohols generally disturb the self-organization of structure-directing agents; thus, the mesostructure of the product tends to be disordered. On the other hand, the co-continuous macroporous structure can be obtained in a limited concentration range of network-forming components. Extreme dilution usually results in the fragmentation and sedimentation of a network-forming phase, as usually observed in the synthesis of powdery mesoporous materials. Recently, a high concentration of surfactant, typically higher than 20 mass %, was also used to prepare monolithic mesoporous materials using a relatively weak interaction between the surfactant and oxide oligomers.⁵ In this case, the long-range mesostructural order is mainly supported by the stable surfactant–cosurfactant–solvent interactions, making the process versatile for fabricating mesoporous devices in larger dimensions.

Numerous trials have been made to organize a highly ordered mesoporous gel network into macroporous assemblies. Some reports demonstrate the successful synthesis of materials with highly ordered mesopores

* Corresponding author. Phone: +8175-383-2411. Fax: +8175 383 2412. E-mail: kazuki@bisco1.kuic.kyoto-u.ac.jp.

† Kyoto University.

‡ National Institute of Science and Technology.

§ K.N. and T.K. are also affiliated with PRESTO, Japan Science and Technology Agency (JST), 4-1-8, Honcho, Kawaguchi City, Saitama 332-0012, Japan.

(1) Kresge, C. T.; Leonowicz, M. E.; Roth, W. J.; Vartuli, J. C.; Beck, J. S. *Nature* **1992**, *359*, 710.

(2) Inagaki, S.; Fukushima, Y.; Kuroda, K. *J. Chem. Soc., Chem. Commun.* **1993**, 680.

(3) Nakanishi, K. *J. Porous Mater.* **1997**, *4*, 67.

(4) Tanaka, N.; Kobayashi, H.; Nakanishi, K.; Minakuchi, H.; Ishizuka, N. *Anal. Chem.* **2001**, *73*, 420A.

(5) Feng, P.; Bu, X.; Pine, D. J. *Langmuir* **2000**, *16*, 5304.

embedded in fibriller gel skeletons that are organized in a macroporous network.^{6,7} The undesired co-presence of short-chain alcohol in the mesostructure-forming stage is avoided either by the modification of starting alkoxide or by selective removal of the alcohol in the deposition process. In either case, however, the precise and systematic control of the macropore structure has not been achieved.

With use of various Si precursors such as tetramethoxysilane, tetraethoxysilane, and bis(trimethoxysilyl)-ethane, amorphous or disordered mesopores with sharp size distribution can be embedded in gel networks which constitute a co-continuous macroporous structure.⁸⁻¹⁰ As a related approach, Smått et al. adopted cationic surfactants (CTAB family) and a nonionic polymer (poly(ethylene glycol)) together, which they call "double-templating synthesis".¹¹ In some cases, there was some indication that at least a part of the material retained highly ordered mesoporous arrangement.¹² In all cases of monolith with well-defined macropores, however, it has never been demonstrated that the highly ordered mesopores that can be evidenced by XRD diffraction could be obtained.

In the present paper we report the following:

1. The compositions including silicon alkoxide, structure-directing agent, water, and acid catalyst, which can spontaneously result in gels with both well-defined macropores and highly ordered mesopores, have been specified.
2. The micelle-swelling agent, an additive that enhances the self-organization of structure-directing agents, has been successfully used to give hierarchical well-defined macropores and highly ordered mesopores.
3. The mesostructural transition, from 2D-hexagonal to mesostructured cellular foam, has been observed in a 3D continuous macroporous gel network, similarly to the case of dispersed precipitates, with an addition of the micelle-swelling agent.

Materials and Methods

Materials Synthesis. The 1,2-bis(trimethoxysilyl)ethane, BTME, was purchased from KIST (Korea Institute of Science and Technology). As a structure-directing agent, poly(ethyleneoxide)-block-poly(propyleneoxide)-block-poly(ethyleneoxide), with an average molecular mass of 5800, was obtained from Aldrich (equivalent to Pluronic P123, BASF). All the solvents and other reagents including 1,3,5-trimethylbenzene, TMB, were purchased from Wako Pure Chemicals Industries, Ltd. and were used as received.

Sample gels were prepared with the starting compositions listed in Table 1 as follows. First, a given amount of P123 was homogeneously dissolved in 0.1 M (M; mol dm⁻³) aqueous solution of nitric acid. In the case that TMB was added to the initial mixture, a given amount of TMB was added to the

(6) Hüsing, N.; Raab, C.; Torma, V.; Roig, A.; Peterlik, H. *Chem. Mater.* **2003**, *15*, 2690.

(7) Zhao, D.; Yang, P.; Chmelka, B. F.; Stucky, G. D. *Chem. Mater.* **1999**, *11*, 1174.

(8) Sato, Y.; Nakanishi, K.; Hirao, K.; Jinna, H.; Shibayama, M.; Melnichenko, Y. B.; Wignall, G. D. *Colloids Surf. A* **2001**, *187/188*, 117.

(9) Nakanishi, K.; Sato, Y.; Ruyat, Y.; Hirao, K. *J. Sol-Gel Sci. Technol.* **2003**, *26*, 567.

(10) Kobayashi, Y.; Nakanishi, K.; Hirao, K. *Mater. Res. Soc. Symp. Proc.* **2004**, *788*, L3.10.1.

(11) Smått, J. H.; Schunk, S.; Linden, M. *Chem. Mater.* **2003**, *15*, 2354.

(12) Shi, Z.-G.; Feng, Y.-Q.; Xu, L.; Da, S.-L.; Ren, Y.-Y. *Microporous Mesoporous Mater.* **2004**, *68*, 55.

Table 1. Starting Compositions, Gelation Time and Resultant Morphology of the Gel Samples in BTME-P123-0.1M HNO₃Aq-TMB System (unit: g)

sample	BTME	P123	TMB	0.1 M HNO ₃ aq	gelation time (min)	morphology
P00E	2.12	0	—	6.07	77	nanoporous
P05E	2.12	0.50	—	6.07	56	nanoporous
P07E	2.12	0.70	—	6.07	59	co-continuous
P09E	2.12	0.90	—	6.07	62	co-continuous
P11E	2.12	1.10	—	6.07	67	co-continuous
P15E	2.12	1.50	—	6.07	72	nanoporous
P19E	2.12	1.90	—	6.07	86	nanoporous
P19E-05	2.12	1.90	0.05	6.07	87	isolated pores
P19E-20	2.12	1.90	0.20	6.07	81	co-continuous
P19E-25	2.12	1.90	0.25	6.07	75	co-continuous
P19E-30	2.12	1.90	0.30	6.07	71	co-continuous
P19E-35	2.12	1.90	0.35	6.07	60	co-continuous
P19E-40	2.12	1.90	0.40	6.07	57	co-continuous

solution and homogenized by vigorous stirring. Then, BTME was added at room temperature under vigorous stirring for hydrolysis. The BTME was immediately hydrolyzed, and after 5 min of stirring, the resultant homogeneous solution was poured into a glass tube. The glass tube was sealed and kept at 60 °C for gelation. The gelation time was determined simply by tilting the sample tube as the time that bulk fluidity of the polymerizing solution was lost. Subsequently, the wet gel was aged at 60 °C for about 5 times the gelation time and evaporation-dried at 60 °C. Residual volatile and organic substances as well as P123 were removed by heat-treating the sample under air from room temperature to 350 °C in 2.5 h and holding at the same temperature for 5 h. The heat-treatment condition was selected so as not to decompose the bridging hydrocarbon chain while removing other organic constituents as completely as possible.¹³

Measurements. The morphology of the dried or heat-treated sample gels was observed by SEM (S-2600N, Hitachi Ltd., Japan, with Pt coating) and FE-SEM (JSM-6700F, JEOL Ltd. without coating).

X-ray powder diffraction (XRD) data were collected at room temperature on a powder diffractometer (MAC Science MXP-3TZ) with vertical θ : θ geometry and Cu K α radiation.¹⁴ Its goniometer has two characteristics to dramatically improve the XRD data in the low 2 θ region: (1) A pair of long Soller slits which improve the diffraction profiles as symmetric as possible and (2) variable-width divergence and scattering slits which suppress the background level. In the present measurements, the variable-width slits were fixed to irradiate sample width at 23 mm.¹⁴

The size distribution of macropores was measured by a mercury porosimetry (PORESIZER-9320, Micromeritics Co., USA), and the size distributions of mesopores were determined by nitrogen adsorption-desorption measurement (ASAP-2010, Micromeritics Co., USA), both with heat-treated gels. For nitrogen adsorption, the pore size distribution was calculated by the BJH method using the adsorption branch of the isotherm.

Results and Discussion

All the gels were obtained as white or translucent monolithic pieces after drying. Some of the resultant gels exhibited typical co-continuous macroporous morphologies depending on the starting composition. The starting compositions, together with respective gelation times and resultant gel morphologies, are listed in Table 1. For the samples without TMB, the gelation time once

(13) Hamoudi, S.; Kaliaguine, S. *Chem. Commun.* **2002**, 2118 (together with electronic supplementary information; <http://www.rsc.org/suppdata/cc/b2/b207134g/>).

(14) Ikeda, T.; Kodaira, T.; Oh, T.; Nisawa, A. *Microporous Mesoporous Mater.* **2003**, *57*, 249.

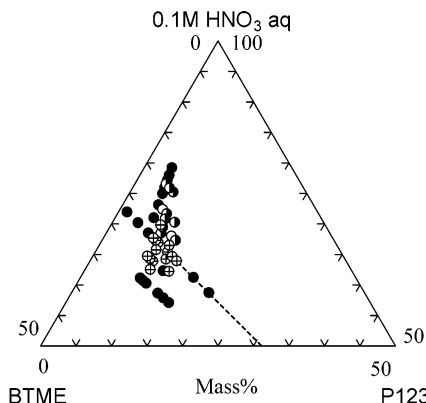


Figure 1. Relation between starting composition and resultant gel morphologies in the BTME-P123-0.1M HNO₃aq system. The dotted line shows the compositions with fixed BTME and 0.1 M HNO₃aq and varied P123 concentration corresponding to the samples PnnE listed in Table 1. Closed circle: nanoporous structure. Crossed circle: co-continuous structure. Open circle: particle aggregates. Half-filled circle: macroscopic two-phases.

decreased with a small amount of P123 addition and then monotonically increased with an increase of added P123. This kind of behavior has been commonly observed in poly(ethylene oxide)-tetraalkoxysilane systems where hydrogen-bonding interaction between the additive polymer and siloxane oligomer is specifically strong.³ Due to the presence of abundant silanol groups on the BTME-derived oligomers and terminal polyoxyethylene chains in P123, a similar kind of interaction between the oligomers and P123 molecules are expected. It is generally recognized in numerous examples that the higher the phase-separation tendency of the polymerizing system, the shorter the gelation time.³ Judging from the morphological evolution described in detail below, the phase-separation tendency passes a maximum between P07E and P11E. It is possible, in the present case, that a substantially high viscosity of P123 dominantly influences the gelation time. With an increase of TMB addition to P19E, on the other hand, the gelation time monotonically decreased. This is simply attributed to the enhanced phase-separation tendency by the addition of TMB as described in detail below.

Figure 1 shows the composition-morphology relationship in the P123-BTME-0.1 M nitric acid pseudo ternary system at 60 °C. Transparent or translucent gels, denoted as filled circles, are obtained when the phase separation to induce micrometer-range domains does not effectively take place until the structure-freezing due to sol-gel transition of the reacting solution. Macroscopic two-phases, consisting of a precipitated gel phase and a supernatant solvent phase, are the result of a much earlier onset of phase separation than the sol-gel transition. Between these extremes, the micrometer-range transient structures of the phase separation (spinodal decomposition in most cases) are frozen-in as permanent morphology of the resultant gels. The transient state of the spinodal decomposition with comparable volume fractions of the conjugate phases typically exhibits a co-continuous structure, where both the gel phase and solvent phase are continuous and highly interconnected. The characteristic size of the structure, domain size, is defined by the sum of the thickness of the (averaged) gel domain and the

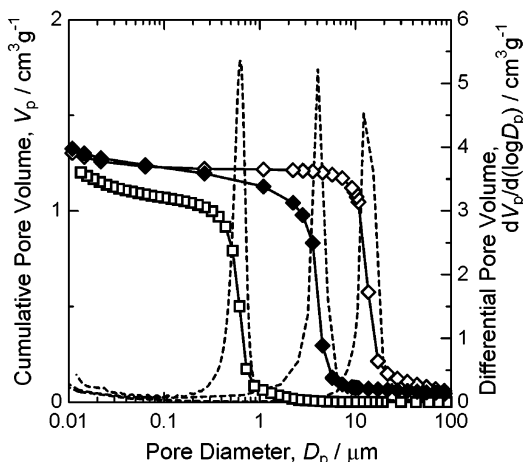


Figure 2. Pore size distribution of heat-treated gel samples measured by the mercury intrusion method. Open diamond: P09E. Closed diamond: P07E. Open square: P19E-25.

width of solvent-phase domains which become macropores after drying.

The results show that concurrent phase separation and sol-gel transition of the polymerizing solution take place with an initial water concentration at around 65 mass %. The figure also indicates that the phase separation occurs earlier than the sol-gel transition in the composition region with water concentration higher than those of the co-continuous structure, which finally results in the "macroscopic two-phases". There are some data points corresponding to the "particle aggregates" morphology, which is between the "co-continuous" and "macroscopic two-phases". On the other hand, an increase in P123 concentration enhances the phase separation to give co-continuous structure with a moderate amount of P123 additions. Further additions of P123, however, lead to the formation of gels without macropores, which indicates that phase separation in the system is suppressed also at higher P123 concentrations (along the dotted line). The dependence of the resultant morphology on P123 concentration is consistent with that of gelation time described above. As has been studied thoroughly, the domain size of the co-continuous structure becomes larger with an increase of the phase-separation tendency of the polymerizing system. In the present case, the domain size can be systematically controlled by adding or reducing either aqueous nitric acid solution or P123 in the starting composition. In addition, the amount of aqueous nitric acid solution controls the volume fraction of micrometer-range pores also. A wide variety of macroporous structures with desired size and volume of micrometer-range pores can be designed by adjusting these two composition parameters. Other parameters such as acid concentration and reaction temperature similarly control the micrometer-range morphology, mainly the domain size, of the gels.

As shown in Table 1, an addition of TMB drastically enhances the phase separation of the P123-BTME-0.1 M nitric acid system. Also in this case, the micrometer-range pores can be controlled similarly to the systems without TMB. Figure 2 shows the pore size distributions determined by Hg porosimetry for the typical macroporous gel samples. In all samples, irrespective of the long-range ordering of the mesopores described below, pores in the micrometer range are

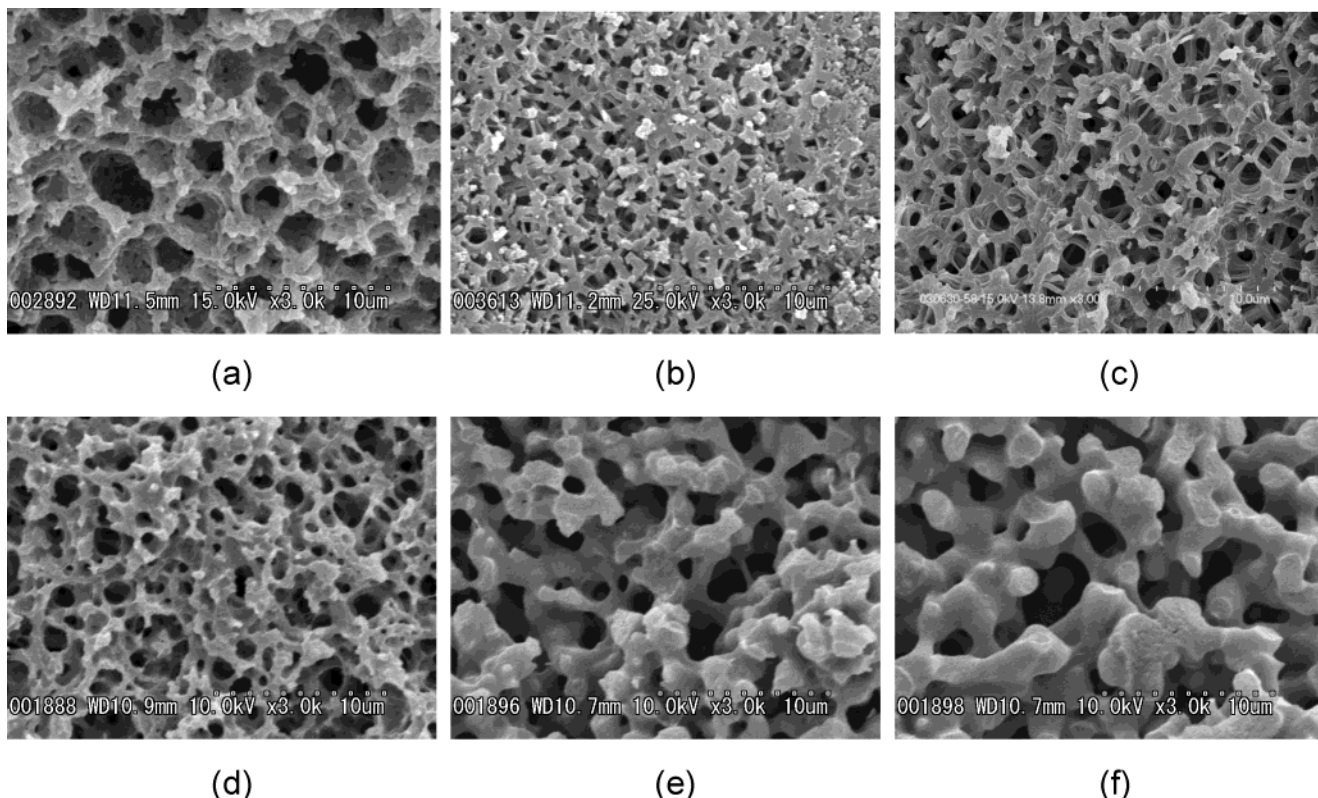


Figure 3. SEM photographs of heat-treated gel samples prepared with varied TMB concentrations. (a) P19E-05, (b) P19E-20, (c) P19E-25, (d) P19E-30, (e) P19E-35, and (f) P19E-40.

sharply distributed. Figure 3 shows selected SEM photographs of the gels prepared with the addition of TMB. With an addition of TMB, the morphology turns from isolated to co-continuous macropores with a fibrous appearance accompanied by the gradual increase in the domain size. Further additions of TMB makes the structure isotropic again accompanied by a slight relative thickening of the gel skeletons. Thus, the morphological evolution with an addition of TMB accompanies a slight anisotropy in the co-continuous macroporous structure in the limited concentration region.

As has been reported earlier on the systems containing tetramethoxysilane^{8,9} or BTME,¹⁰ the co-continuous macroporous gels prepared with P123 surfactant retain sharply distributed mesopores evidenced by nitrogen adsorption measurement. Figure 4 shows adsorption isotherms and corresponding pore size distributions of the gels shown in Figure 3. With addition of TMB < 3% by mass to P123, drastic changes both in isotherm and in pore size distribution can be recognized. After addition, the adsorption branch exhibits a distinct inflection corresponding to sharper pore size distribution, which can be confirmed in the corresponding differential pore size distribution curves. The overall shape of the adsorption-desorption hysteresis loop turns from H2 to H1 of IUPAC classification. The type H2 hysteresis is observed in many inorganic oxide gels with interconnected networks of pores with variations in their size and shape, while the type H1 is commonly observed in adsorbents with a sharp distribution of uniform-shaped pores including MCM-41 type highly ordered mesoporous materials. From these data, the addition of a small amount of TMB is assumed to enhance the self-organization of P123 to transform the pore system from

random to cylindrical in shape without significantly affecting the median pore size.

The overall structural changes including both pores and walls should be evaluated by XRD measurements. The remarkable sharpening in XRD profiles of the samples with additions of TMB shown in Figure 5a indicates that significant ordering of the mesopores takes place by the addition of TMB. This agrees well with the enhanced ordering of mesopores by the addition of butanol to bis(triethoxysilyl)ethylene-P123-TMB gels under strongly acidic conditions.¹⁵ From 0.05 to 0.20 g addition of TMB, the overall features of the adsorption isotherms as well as the XRD diffraction profiles remained unchanged, except for the systematic shifts of median pore size or main peak position.⁵ The sharp first peak is assumed to be the (10) diffraction of 2D-hexagonal symmetry. The weak higher order diffractions around corresponding (20) and (11) positions suggest that the gels retain a large fraction of highly ordered mesopores. Figures 6a and 6b show FE-SEM images of fractured surfaces of the macroporous gels. Well-aligned 2D-hexagonal pores can be recognized throughout the cross section of the gel skeletons.

Further addition of TMB beyond 0.20 g leads to an additional structural transformation. It can hardly be recognized in the nitrogen adsorption data except for a slight increase in the median pore size. The XRD profiles of P19E-20 and P19E-25, however, essentially differ from each other (Figure 5b). Although the main diffraction of P19E-25 is expected to shift to a lower angle due to the swelling of P123 micelles by increased

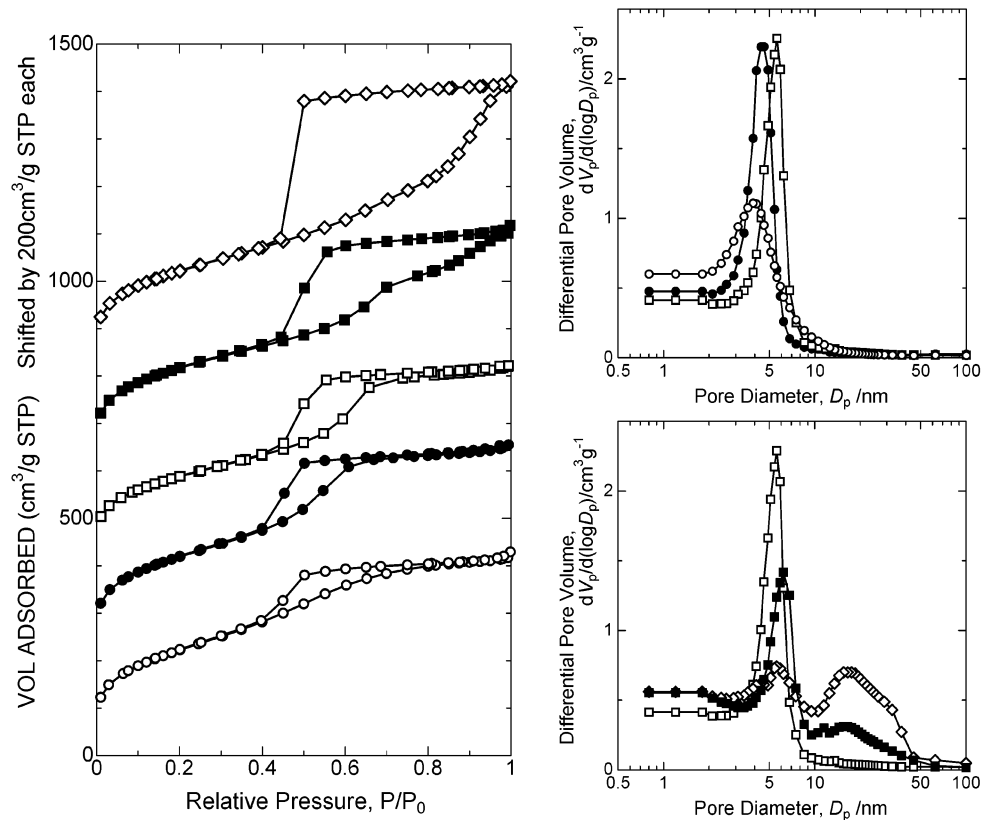


Figure 4. Nitrogen adsorption isotherms and corresponding pore size distribution curves by the BJH method for the heat-treated gel samples. Open circle: P19E. Closed circle: P19E-05. Open square: P19E-25. Closed square: P19E-30. Open diamond: P19E-40.

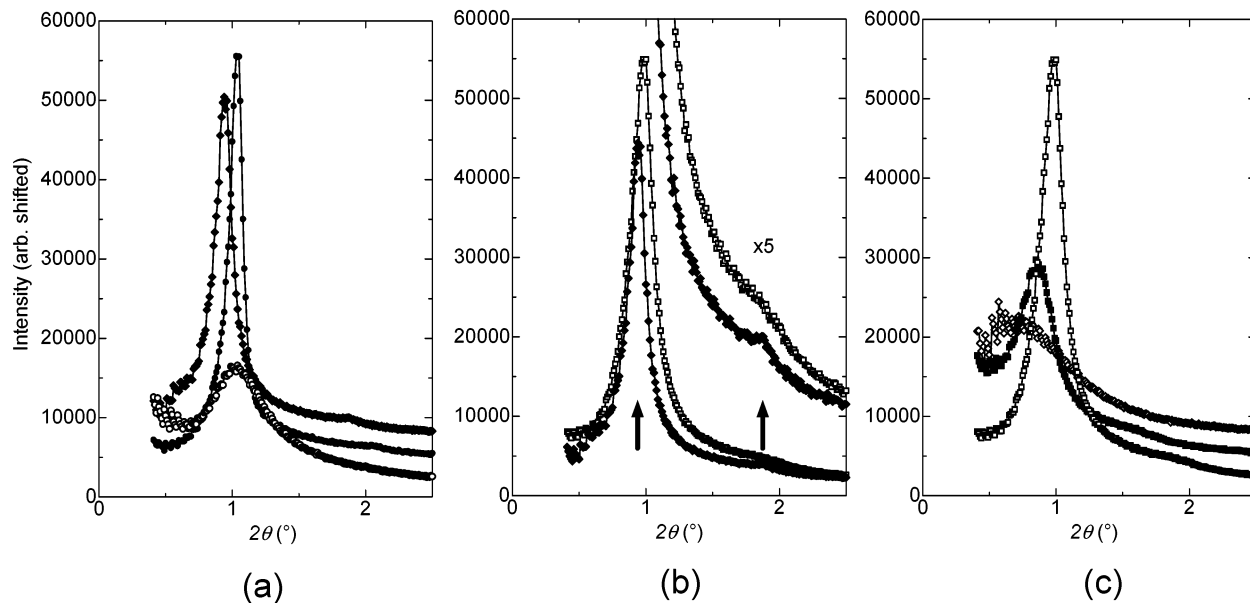


Figure 5. X-ray diffraction profiles of heat-treated gel samples prepared with varied TMB concentrations. (a) Amorphous (P19E: open circle) to 2D-hexagonal symmetry (P19E-05, closed circle, and P19E-20, closed diamond). (b) 2D-hexagonal (P19E-20) to other symmetry (P19E-25: open square); inserted left and right arrows respectively indicate (10) and (20) diffractions corresponding to d spacing of 9.39 nm. (c) Evolution into mesostructured cellular foam (P19E-30, closed square, and P19E-40, open diamond).

TMB (also evidenced by nitrogen adsorption), the apparent peak top shifts slightly to a higher angle accompanied by a substantial increase in the fwhm. In addition, the higher order diffractions become broader with a slight shift toward the lower angle. According to Inagaki et al.,¹⁶ mesopores in BTME-derived gels tem-

plated by cationic surfactant can exhibit 2D-hexagonal as well as 3D-hexagonal symmetry. In the 3D-hexagonal arrangement, the (100) diffraction is superposed by

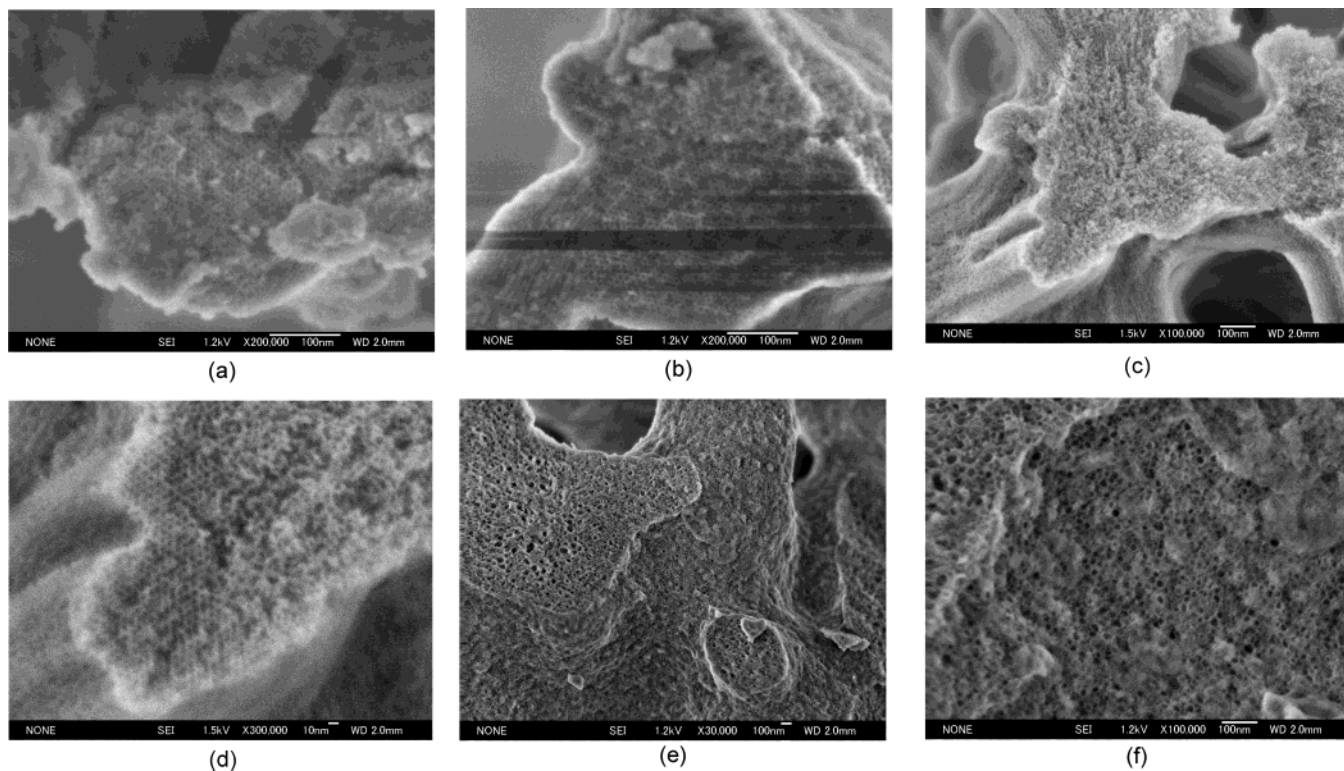


Figure 6. FE-SEM photographs of heat-treated gel samples prepared with varied TMB concentrations. (a) P19E-05, (b) P19E-20, (c) P19E-25, (d) P19E-25 (higher magnification), (e) P19E-40, and (f) P19E-40 (higher magnification).

strong (002) and (101) diffractions that have peaks at slightly higher angles than that of (100). In this case, the higher order diffractions such as (110), (103), and (112) are found at lower angles than those of (20) and (11) in 2D-hexagonal geometry. Alternatively, according to the *in situ* XRD study on the mesophase transformation with temperature, the profiles of structurally related MCM-41 (2D-hexagonal) and MCM-48 (cubic) structures give strongest peaks corresponding to (10) and (211) diffractions, respectively, the latter being located at a slightly higher angle.¹⁷ It is, therefore, possible that the present macroporous gels with BTME-P123-TMB composition exhibit a transient mesoporous arrangement either in 3D-hexagonal or cubic symmetry at the moderate TMB concentration. Figures 6c and 6d show FE-SEM images of a fractured surface of P19E-25 gel sample at different magnifications. The 2D-hexagonal arrangement can be recognized mainly in the peripheral parts of the co-continuous gel skeletons. Although the core parts appear fairly disordered, they must have significant contribution to give intense overall XRD diffractions, which means there exist at least high mesoscale correlation over the substantial length scale. The detailed structural order in the core parts will be made clear by additional TEM and electron diffraction measurements.

At higher TMB concentrations than 0.25 g, the structural order of mesopores is readily lost under XRD (Figure 5c). In parallel, the nitrogen adsorption isotherm deforms to exhibit a broader hysteresis loop of type H2 with an increased adsorption volume in a higher relative pressure region. In the corresponding differential pore size distribution, the second maximum at around 20–

30 nm emerges and grows with an increase of TMB concentration. At the highest TMB concentration adopted in the present study, the structural order detectable by XRD is completely lost. The inspection by FE-SEM of the P19E-40 sample (Figures 6e and 6f) revealed that the mesopores are very similar to those known as “mesostructured cellular foam”, MCF, reported in detail for precipitated mesoporous silica.^{18,19} Their sizes are in excellent agreement with those estimated by nitrogen adsorption (adsorption branch). Provided that the “window size” can be estimated by the desorption branch, all the gels in the present BTME-P123-TMB system exhibit almost identical window size irrespective of the amount of added TMB. The mesostructural transition from 2D-hexagonal to MCF has been rationalized in the TEOS-P123-TMB precipitate system by considering the interfacial energy requirements of micelles swollen by TMB.²⁰ From the morphological evolution with TMB addition described above, the interactions among P123, TMB, and BTME- or TEOS-derived oligomers are assumed to be essentially similar to each other in both systems. If the formation of noded and subsequently spheroidized structure of the cylindrical micelles, proposed by Lettow et al., is involved in the mesostructural transformation, it is possible for the transient spheroidized (not yet highly swollen) micelles to pack into HCP symmetry without significantly changing the micelle diameter.

(18) Schmidt-Winkel, P.; Lukens, W. W., Jr.; Yang, P.; Margolese, D. I.; Lettow, J. S.; Ying, J. Y.; Stucky, G. D. *Chem. Mater.* **2000**, *12*, 686.

(19) Schmidt-Winkel, P.; Glinka, C. J.; Stucky, G. D. *Langmuir* **2000**, *16*, 356.

(20) Lettow, J. S.; Han, Y. J.; Schmidt-Winkel, P.; Yang, P.; Zhao, D.; Stucky, G. D.; Ying, J. Y. *Langmuir* **2000**, *16*, 8291.

Although both the hexagonally aligned pores and those in the MCF structure are fully accessible by nitrogen in the bulk form, the 2D-hexagonal pores run parallel to the skeleton length possibly due to the tensile stress exerted during the coarsening process of the co-continuous domains. The macroporous materials with MCF-type mesopores, on the other hand, will be better accessed directly from the macropore regions and favored for the separation of high molecular-mass compounds especially in biochemistry fields.²¹ Since the MCF structure is based on a stable microemulsion in the P123–alcohol–TMB system, and the parameters controlling the micelle size are well-investigated,¹⁸ it will be highly possible to control the structural features of macropores and of embedded mesopores independently. The advantage of completely spontaneous formation of hierarchical mesopores and macropores is its versatility to prepare porous structures in miniaturized and/or confined spaces. Once the reaction solution is introduced, highly permeable and efficient liquid contact devices can be prepared within the spaces in any size and any shape.

Analogous spontaneous formation of hierarchical macro–mesoporous structure has been confirmed also in the systems containing tetraalkoxysilanes or other bis(trialkoxysilyl)alkanes as a Si source, or other non-ionic or ionic surfactants as a structure-directing agent. Details of these family compounds will be published elsewhere.

(21) Zhao, J.; Gao, F.; Fu, Y.; Jin, W.; Yang, P.; Zhao, D. *Chem. Commun.* **2002**, 752.

Conclusion

Polymerization-induced phase separation in the course of sol–gel transition of the BTME-based system in the presence of P123 resulted in the formation of hierarchical mesoporous and macroporous materials. The addition of TMB significantly stabilized the cylindrical micelles of P123, leading to the emergence of long-range order in the mesoporous arrangement. Further additions of TMB induced additional structural transformation from 2D-hexagonal, through possibly 3D-hexagonal, to mesostructured cellular foam, MCF, with relatively narrow pore size distribution. The integration of highly ordered mesopores into homogeneously accessible macroporous arrays can be achieved through the completely spontaneous chemical process. Miniaturized macro–mesoporous devices in various shapes will find a broad range of application fields such as separation science, sensing, and supports for catalysts or biocatalysts.

Acknowledgment. Technical assistance of JEOL Ltd. for FE-SEM operation is gratefully acknowledged. Financial support by a Grant-in-Aid for Scientific Research (No. 15206072) from the Ministry of Education, Culture, Sports, Science and Technology, Japan, is gratefully acknowledged. Also, this work is partially supported by the 21st century Center Of Excellence (COE) program, COE for a United Approach to New Material Science, which is financially supported by the Ministry of Education, Culture, Sports, Science and Technology, Japan.

CM049320Y